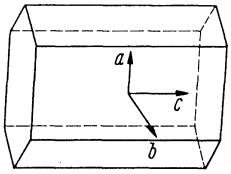

Fig. 30A-2-001. KNO_3. Crystal form grown from aqueous solution [65Saw]. *a*, *b*, *c* correspond to the crystalline axes in phase II.

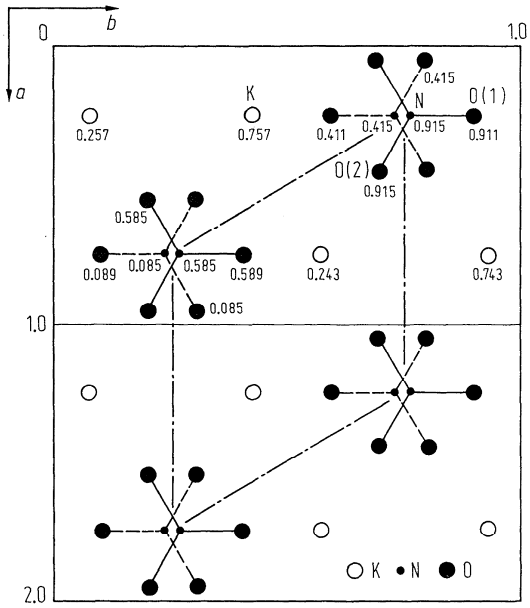

Fig. 30A-2-002. KNO_3. Structure of phase II [76Nim]. The pseudohexagonal cell is shown by dashed-dotted lines. The figure is drawn by the reported fractional coordinates at 25 °C in [73Nim]. K atoms lie on 4 sets of planes, parallel to the *ab* face of each unit cell. See Table 30A-2-003.

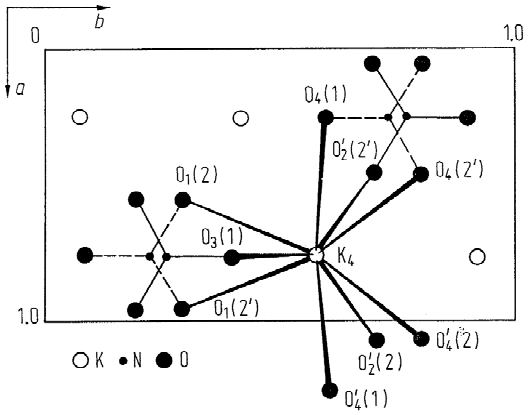

Fig. 30A-2-003. KNO_3. Structure of phase II [73Nim]. Projection along the *c* axis.

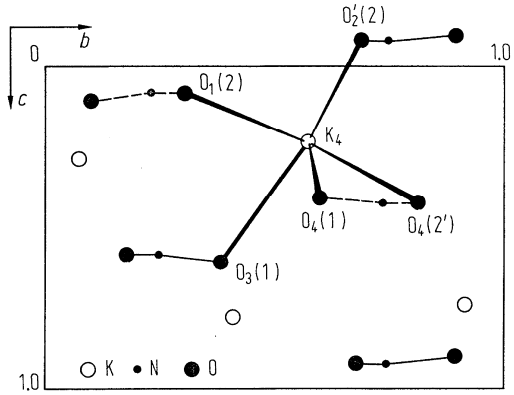

Fig. 30A-2-004. KNO_3. Structure of phase II [73Nim]. Projection along the *a* axis.

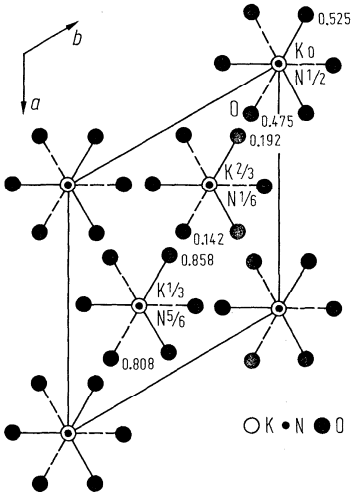

Fig. 30A-2-005. KNO_3. Structure of phase I [76Nim]. Projection along the hexagonal *c* direction. NO_3 on each site is in dynamical disorder between two oritentations. Numbers in figure indicate fractional coordiante *z* at 151 °C.

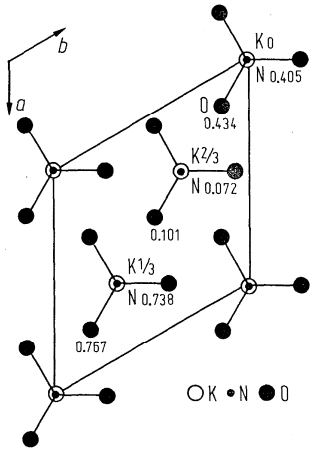

Fig. 30A-2-006. KNO_3. Structure of phase III [76Nim]. Projection along the hexagonal *c* direction. Numbers in figure indicate fractional coordinate *z* at 91 °C.

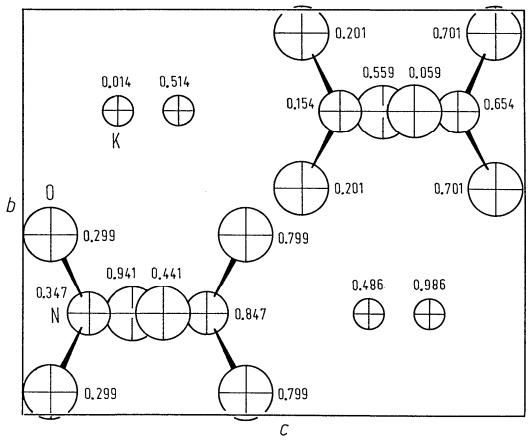

Fig. 30A-2-007. KNO_3. Structure of high pressure phase IV [86Wor]. p = 0.36 GPa, T = RT. Projection along the a axis. The numbers represent x coordinates of atoms. N–O bonds are drawn.

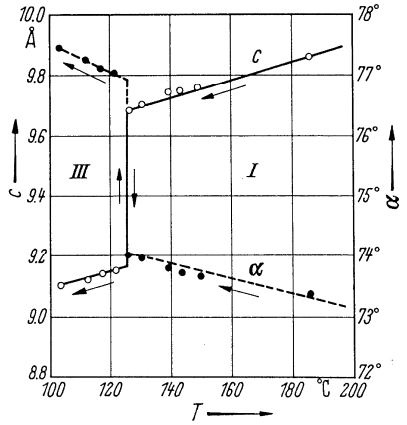

Fig. 30A-2-008. KNO_3. α, c vs. T [65Kaw]. α: trigonal angle. c: hexagonal unit cell parameter.

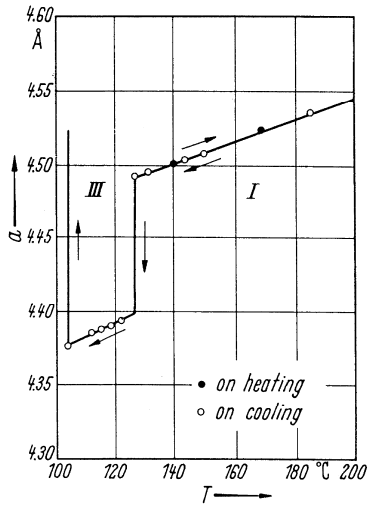

Fig. 30A-2-009. KNO_3. a vs. T [65Kaw]. a: trigonal unit cell parameter.

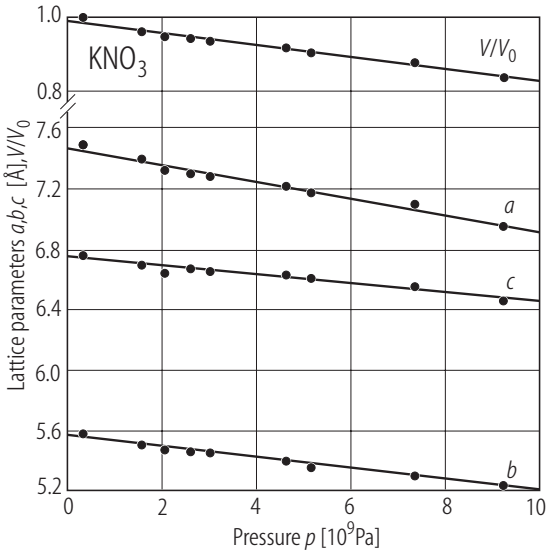

Fig. 30A-2-010. KNO_3. a, b, c, V/V_0 vs. p [88Ada]. T = RT. V: unit cell volume, V_0: unit cell volume at zero pressure.

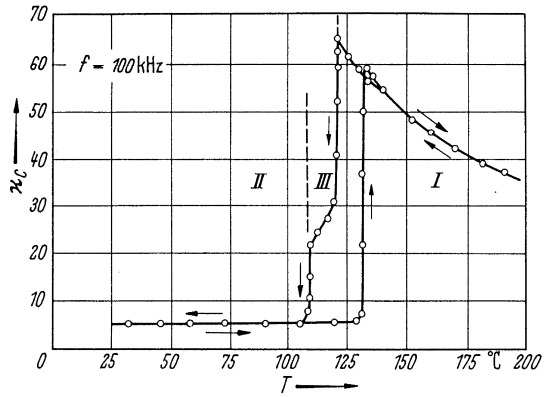

Fig. 30A-2-011. KNO_3. κ_a, κ_b, κ_c vs. T [61Saw].

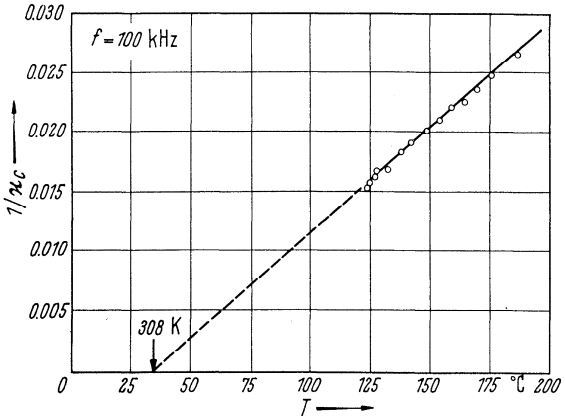

Fig. 30A-2-012. KNO_3. $1/\kappa_c$ vs. T [61Saw].

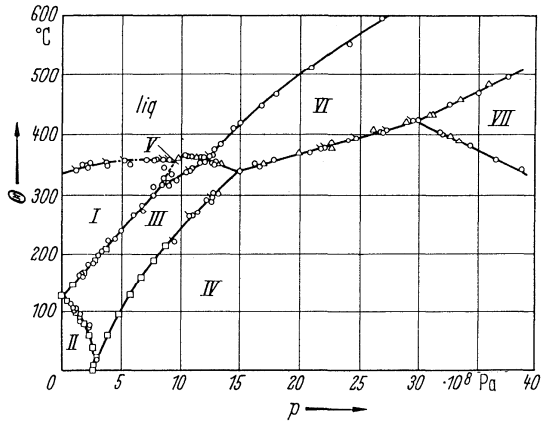

Fig. 30A-2-013. KNO_3. Θ vs. p [65Rap].

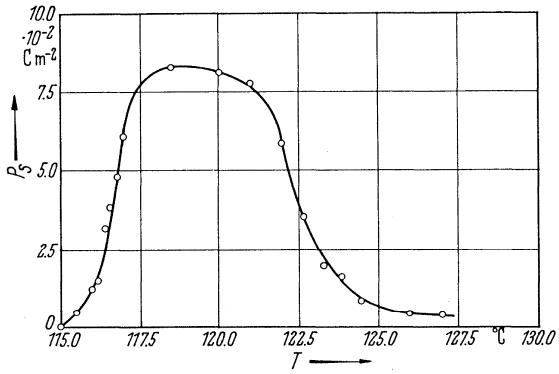

Fig. 30A-2-014. KNO_3. P_s vs. T [61Saw].

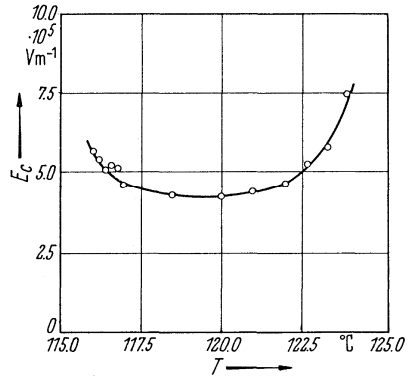

Fig. 30A-2-015. KNO_3. E_c vs. T [61Saw].

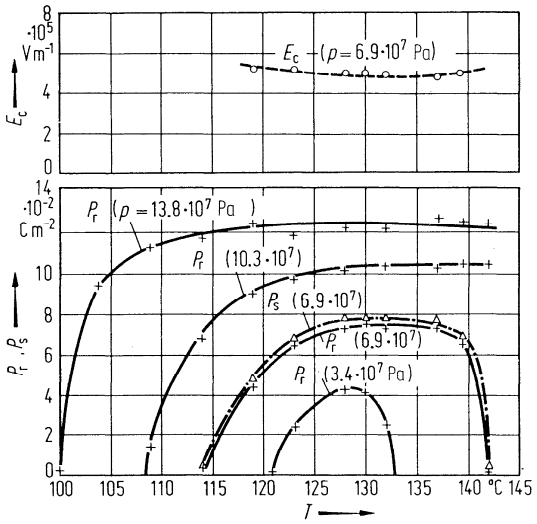

Fig. 30A-2-016. KNO_3. P_s, P_r, E_c vs. T [68Tay]. Parameter: p. P_r: remanent polarization. As to the reproducibility, see [71Mid].

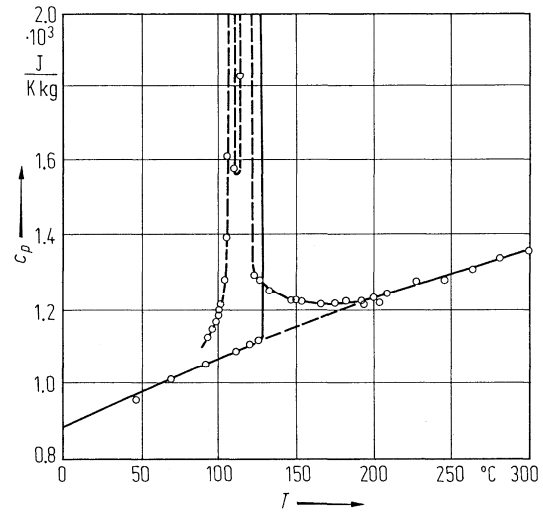

Fig. 30A-2-017. KNO_3. c_p vs. T [41Mie]. Full line: on heating. Dashed line: on cooling.

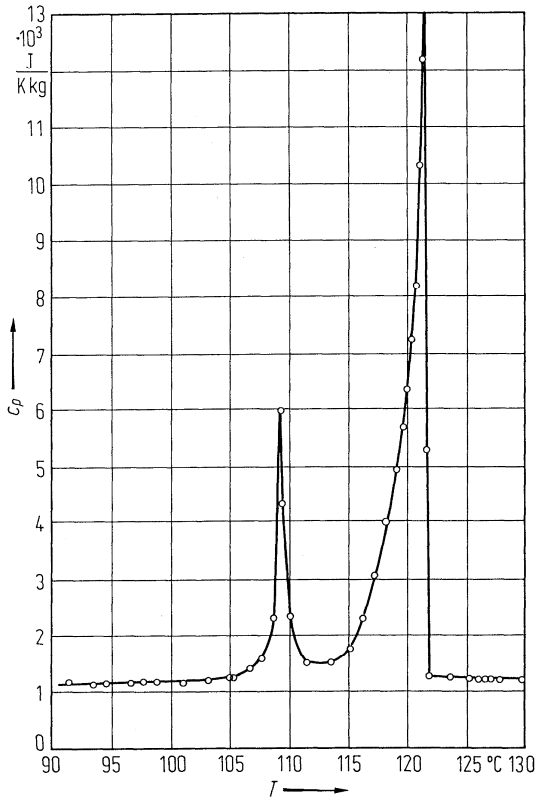

Fig. 30A-2-018. KNO_3. c_p vs. T in the vicinity of I–III–II transitions [41Mie].

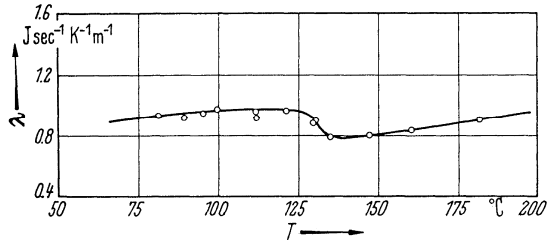

Fig. 30A-2-019. KNO_3 (polycrystal). λ vs. T [60Yos]. λ: thermal conductivity.

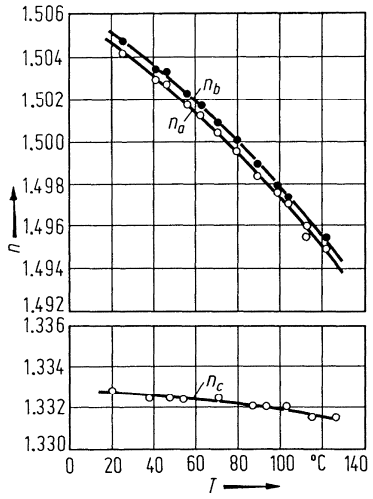

Fig. 30A-2-020. KNO_3. n_i vs. T [68Yan].

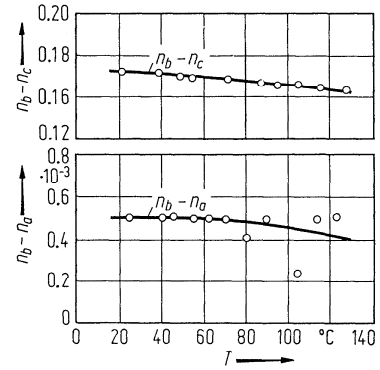

Fig. 30A-2-021. KNO_3. $n_b - n_a$, $n_b - n_c$ vs. T [68Yan].

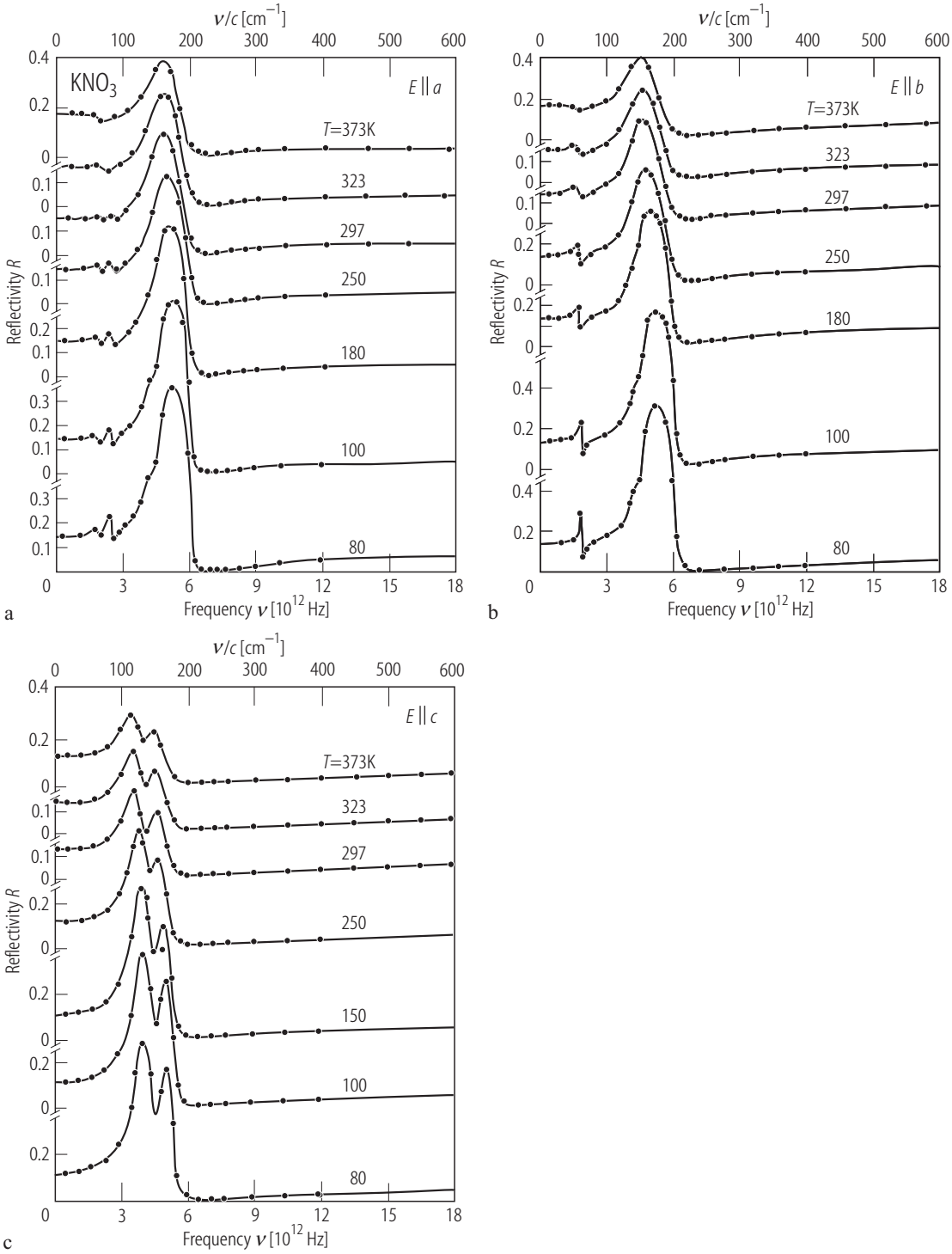

Fig. 30A-2-022. KNO_3. R vs. ν in phase II [88Bre]. Parameter: T. (**a**) $\boldsymbol{E} \parallel \boldsymbol{a}$, (**b**) $\boldsymbol{E} \parallel \boldsymbol{b}$, (**c**) $\boldsymbol{E} \parallel \boldsymbol{c}$. R: far infrared reflectivity.

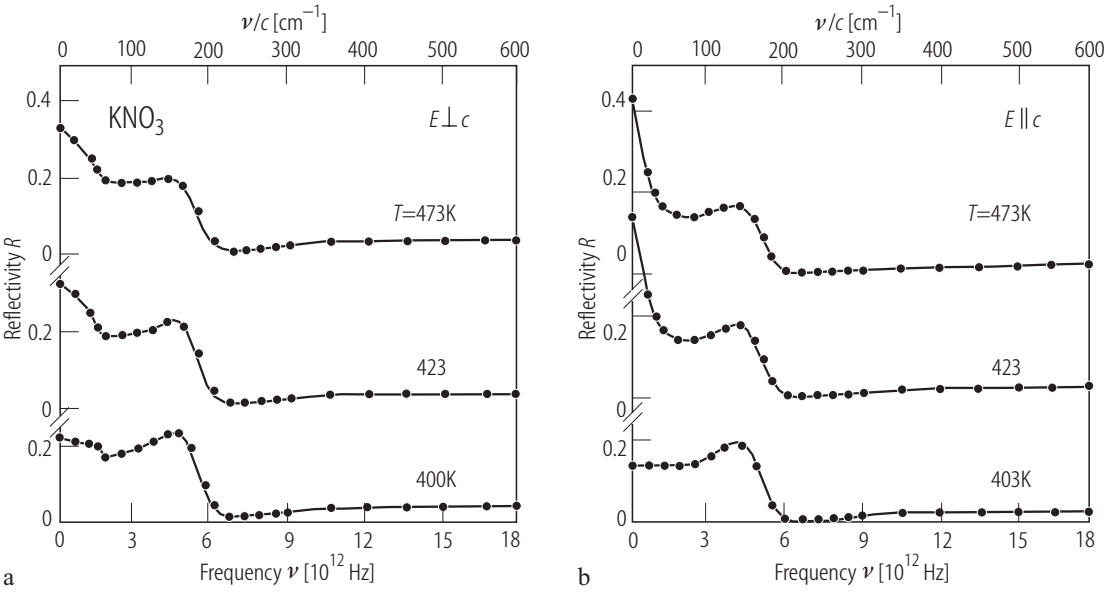

Fig. 30A-2-023. KNO_3. R vs. ν in phase I [88Bre]. Parameter: T. (**a**) $\boldsymbol{E} \perp \boldsymbol{c}$, (**b**) $\boldsymbol{E} \parallel \boldsymbol{c}$. R: far infrared reflectivity. $\boldsymbol{c}$: unit cell vector in hexagonal lattice.

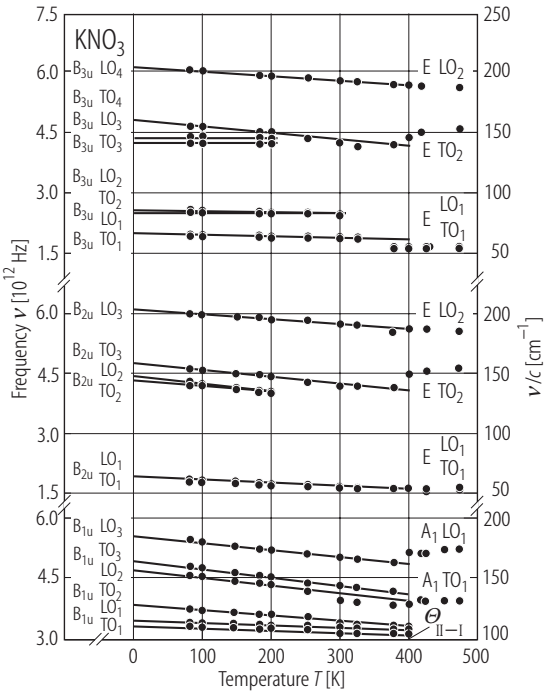

Fig. 30A-2-024. KNO_3. ν vs. T [88Bre]. ν: lattice mode frequency measured by far infrared spectroscopy.

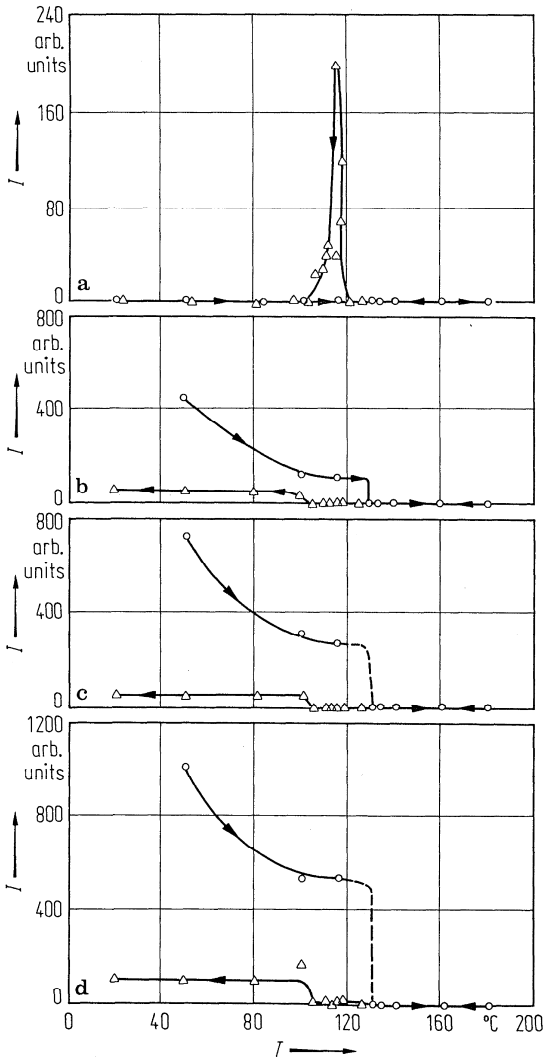

Fig. 30A-2-025. KNO_3. *I* vs. *T* for several phonon modes [68Bal]. *I*: Raman scattering intensity. (**a**) line at 120 cm^{-1}, (**b**) line at 83 cm^{-1} performed with the geometry of *Y*(*ZY*)*X*, (**c**) line at 83 cm^{-1} performed with the geometry of *Y*(*XZ*)*Y*, (**d**) line at 50 cm^{-1}. Circles: on heating, triangles: on cooling.

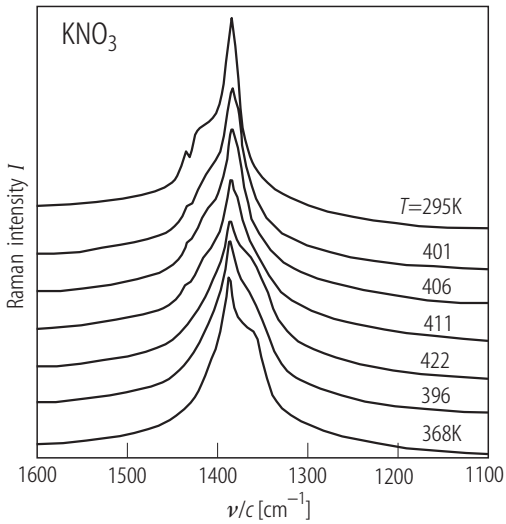

Fig. 30A-2-026. KNO_3. I vs. ν/c for ν_2 mode [92Har]. Parameter: T. I: Raman intensity. ν: frequency of Raman scattering. Temperature was changed from RT (phase II) to 422 K (phase I), then cooled down to phase III (396 K, 368 K).

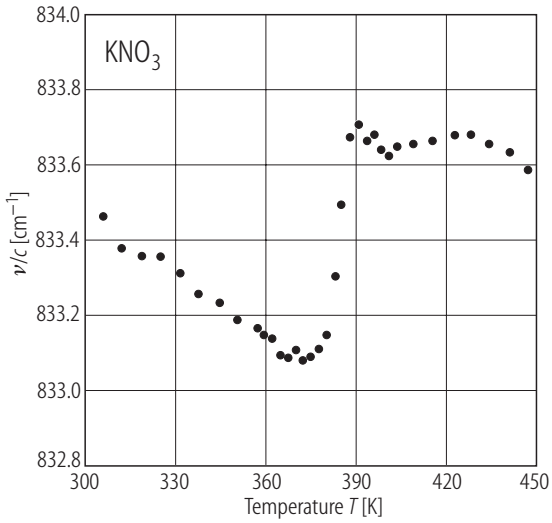

Fig. 30A-2-027. KNO_3. ν/c vs. T [92Har]. ν: frequency of Raman scattering. On cooling. The I-III transition takes place at about 390 K.

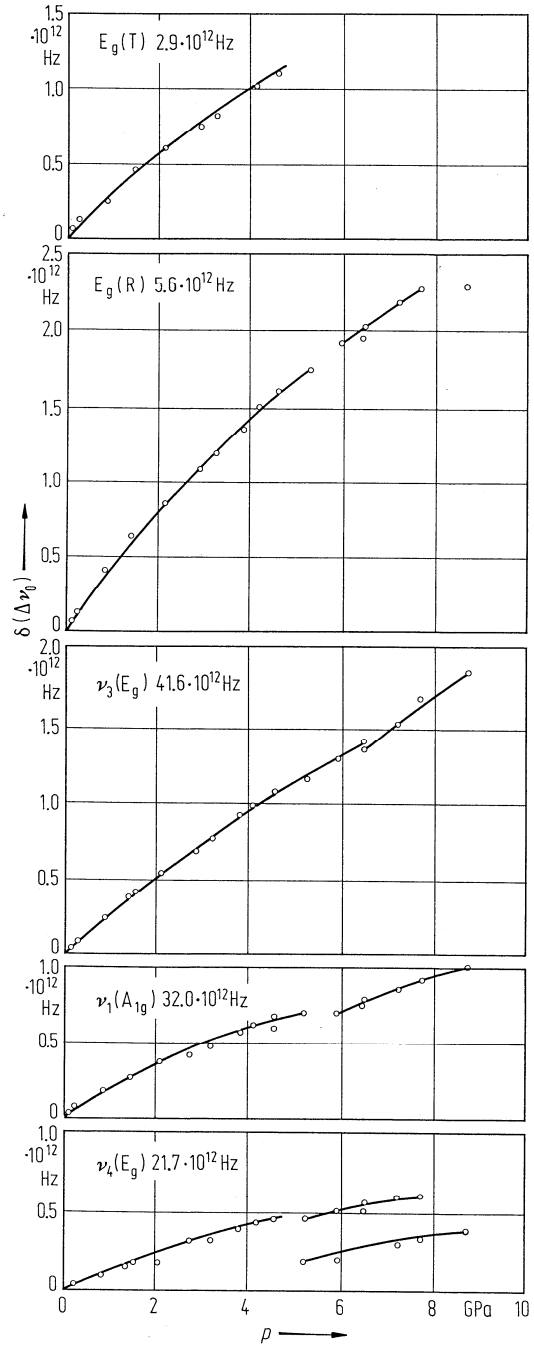

Fig. 30A-2-028. KNO_3. $\delta(\Delta\nu_0)$ vs. p [81Ada]. T = 293 K. $\delta(\Delta\nu_0)$: change in Raman shift. Raman shifts at 0 GPa are described in figures.

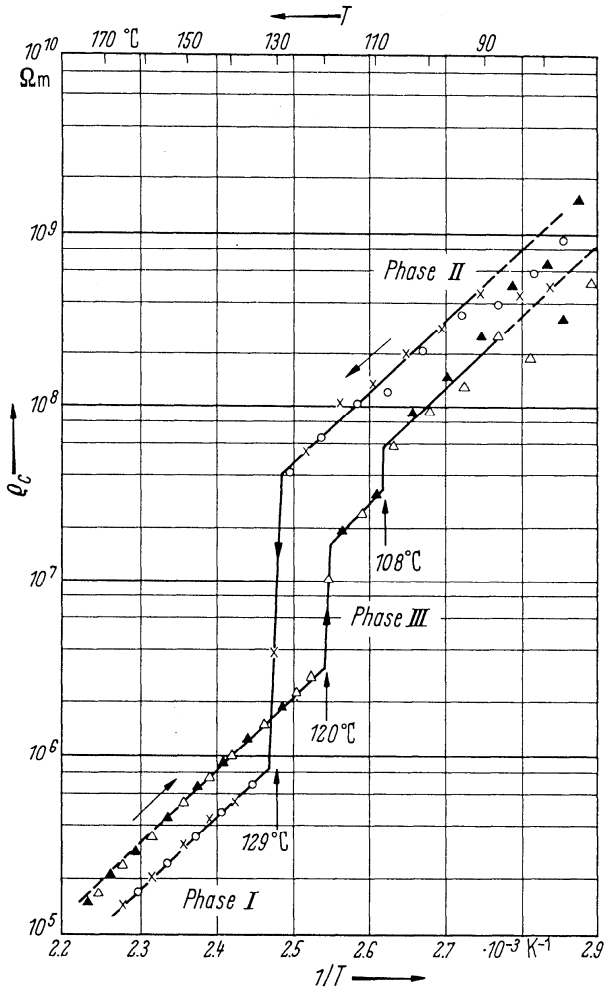

Fig. 30A-2-029. KNO_3. ρ_c vs. $1/T$ [62Asa].

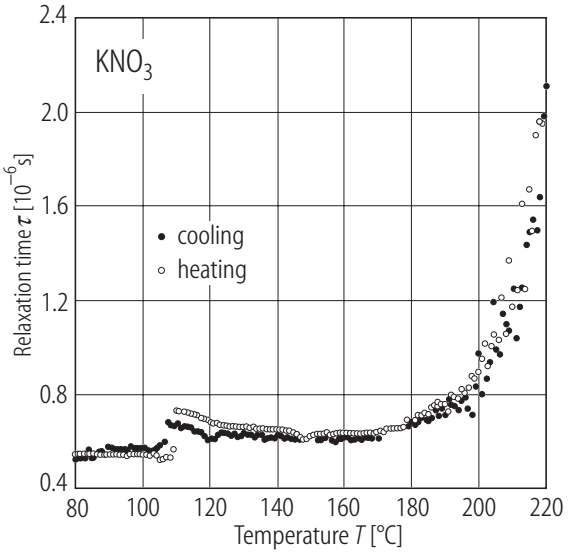

Fig. 30A-2-030. KNO_3. τ vs. T [90Kaw]. τ: relaxation time derived from the frequency dependence of complex electrical conductivity along the *c* axis.

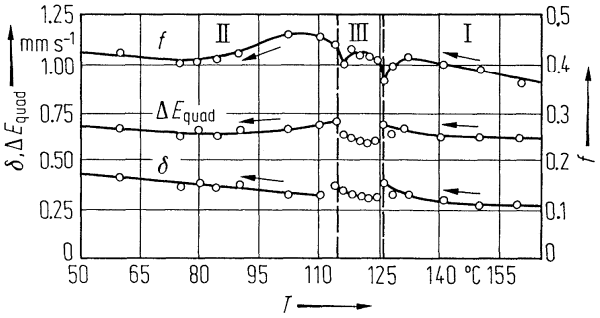

Fig. 30A-2-031. KNO_3. δ, ΔE_{quad}, f vs. T [68Lig]. δ: isomer shift, ΔE_{quad}: quadrupole splitting, f: Debye-Waller factor for ^{57}Co in KNO_3.

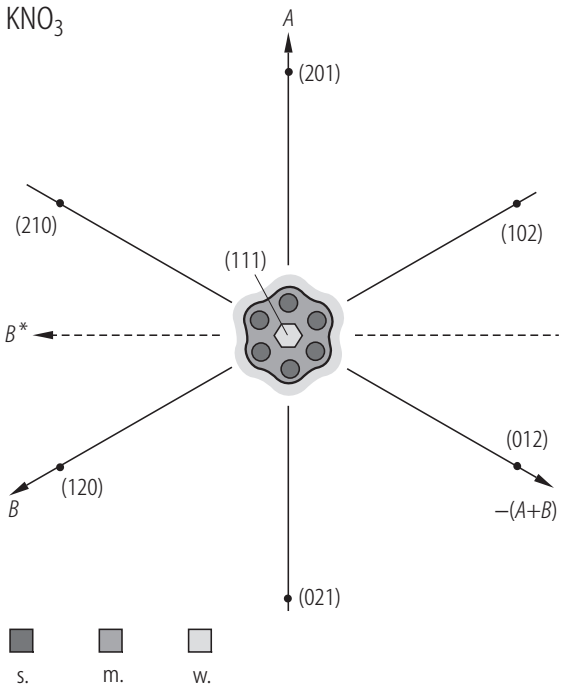

Fig. 30A-2-032. KNO_3. Intensity distribution of X-ray diffuse scattering around the (111) reciprocal lattice point [62Shi]. T = 130 °C. s, m, w: strong, medium, weak intensity region, respectively. A, B are the axes of the hexagonal unit cell.

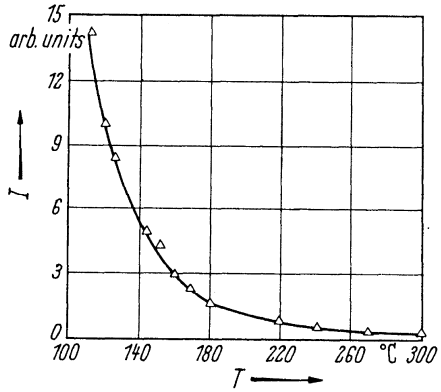

Fig. 30A-2-033. KNO_3. I vs. T [62Shi]. I: intensity of X-ray diffuse maximum in the vicinity of (111).

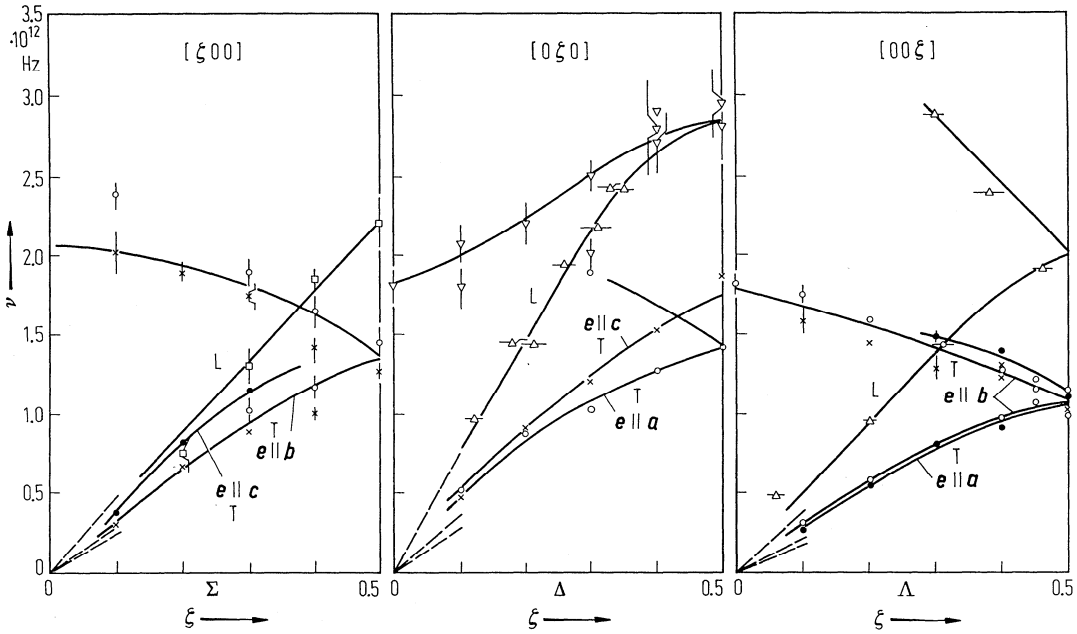

Fig. 30A-2-034. KNO_3. ν vs. ζ [78Rao]. T = RT. ν: phonon frequency, ζ: reduced wave vector coordinate, $\boldsymbol{e}$: polarization vector. Dashed lines indicate initial slopes of phonon branches estimated from sound velocities.

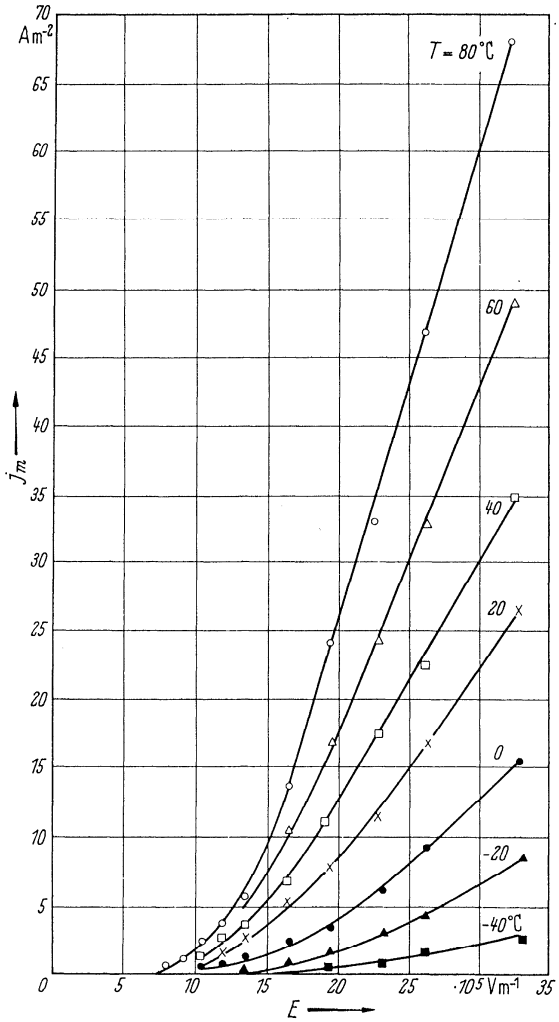

Fig. 30A-2-035. KNO_3 (polycrystal). j_m vs. E [64Dor]. Parameter: T. j_m: maximum switching current density.

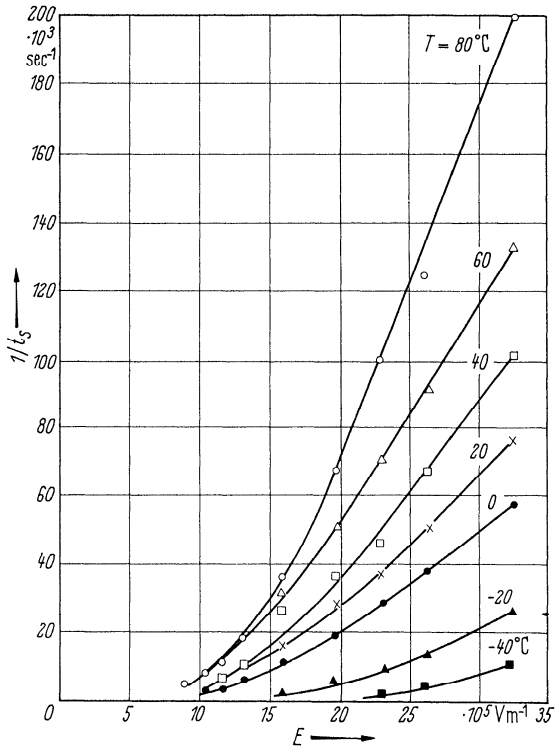

Fig. 30A-2-036. KNO_3 (polycrystal). $1/t_s$ vs. E [64Dor]. Parameter: T. t_s: switching time.